Evaluation of Deep Learning Techniques for Motion Artifacts Removal

Alessandro Sciarra[1,2], Soumick Chatterjee[2,3], Max Dünnwald[1,4], Oliver Speck[2,5,6,7], and Steffen Oeltze-Jafra[1,5,6]

[1]MedDigit, [2]BMMR, [3]DKE, [4]INF-OVGU, [5]CBBS, [6]DZNE-Magdeburg, [7]LIN-Magdeburg

Problem Description

Motion artifacts are still an open problem in research and clinical routine MR acquisitions [3, 5, 6, 7, 8, 9]. In this work, we comparatively evaluated the performance of two neural networks for the task of motion artifacts removal.

Methods

Two datasets were compiled using first, the T1-weighted (T1-w) images from the IXI clinical neuroimaging repository and second, the 2D SheppLogan phantom, Fig. 2.

Moreover, two neural networks were utilized: Pix2pix [4] and a ResNet-based network, originally proposed for undersampled MRI reconstruction [1]. Motion artifacts were artificially created using a custom-made Python function. The pix2pix network was configured with a U-Net generator and a PatchGAN discriminator, code. Our ResNet uses a modified version of the Residual Block, by adding a Spatial Dropout. For Pix2Pix, the dataset contained 2000/1000/1000 paired samples (corrupted & ground truth), for training, validation, and testing, respectively. For ResNet, the dataset contained only the central slices of each volume, from the 60th to the 90th slice, of 100/35/50 subjects (3100/1085/1550 images), for training, validation and testing, respectively. For initial tests using ResNet (ResNet-1), one random angle was chosen for each slice, and all the lines of that particular slice were rotated using that same angle. For the second test using ResNet (ResNet-2) and for the pix2pix test, images were synthetically corrupted in the same manner. The obtained results were analyzed by calculating the mean-squared-error (MSE). Furthermore, after skull-stripping and three tissues segmentation (gray matter, GM, white matter, WM and cerebrospinal fluid, CSF) performed using FSL , a multi-class DICE coefficient [2] and volume ratios were calculated. The volume ratio is computed by dividing the number of pixels of each tissue class, e.g., the number of pixels for GM in the predicted image, by the number of pixels of the same class in the ground-truth image. The processing pipeline is shown in Fig. 1.

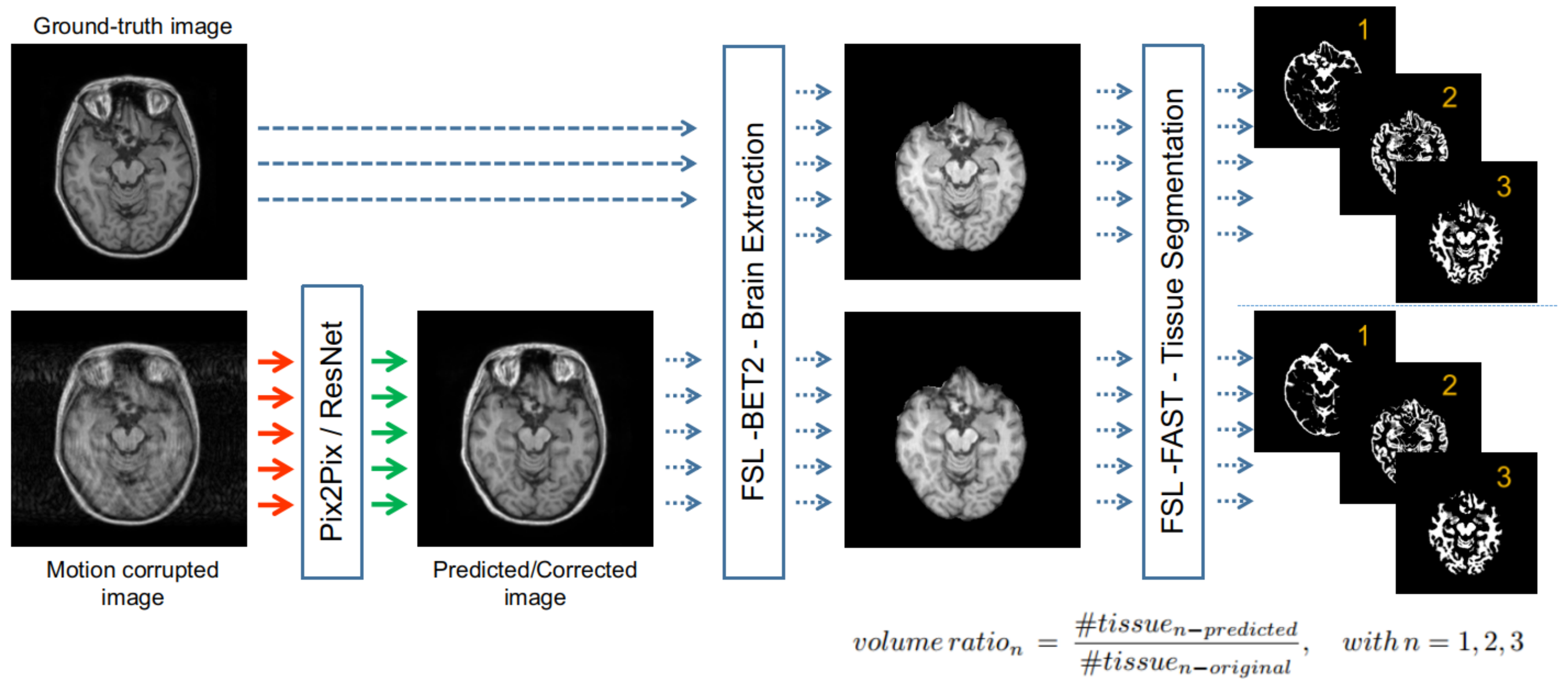

Fig. 1: Pipeline used for processing the results

Program number 3370

Results

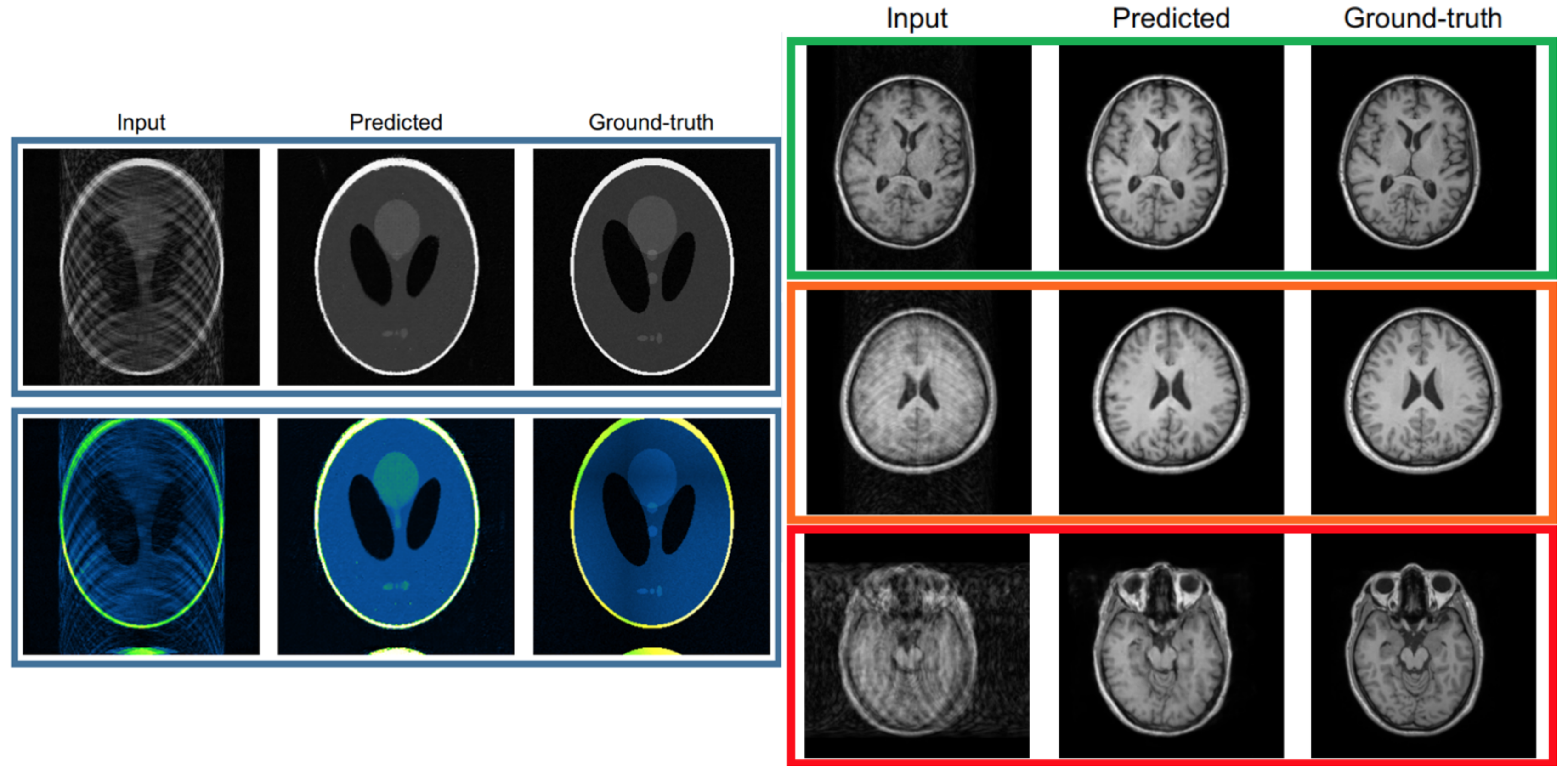

Fig. 2: **LEFT SIDE:** Motion correction using Pix2Pix for Sheep-Logan phantom. Upper row: Input) Sheep-Logan phantom corrupted with artificial motion artifacts, Predicted) image obtained from Pix2Pix, Ground-truth) original image without motion artifacts. Bottom row: similar to the upper row, but with additional inhomogeneities. **RIGHT SIDE:** Classification into three main scenarios. Upper row: input image slightly corrupted by motion artifacts. Middle row: input image with medium level of corruption. Bottom row: input image heavily corrupted by motion artifacts, even large structures are not easy to recognize.

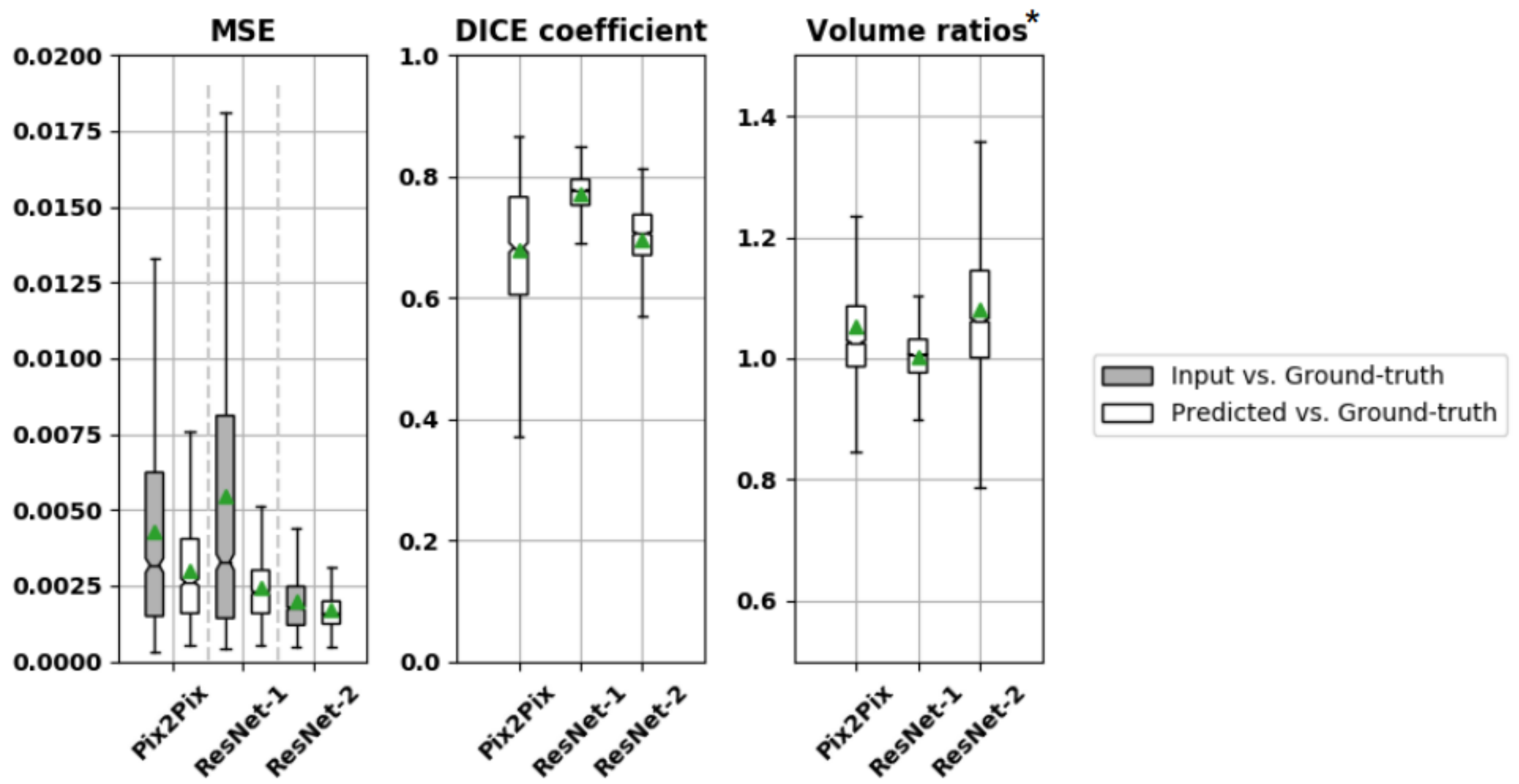

Fig. 3: Results: Mean-squared-error (MSE), DICE coefficient and Volume ratios. The green triangles indicate the mean values and the lines the corresponding median values. The MSE values, are calculated first, between input (corrupted image) and ground-truth (free-motion image) and second, between the predicted/corrected and the ground-truth image. The DICE coefficients are computed in a similar fashion. In this case, the values are the averages across the three considered classes GM, WM and CSF. The last box plot shows the volume ratios, also, averaged across the three classes. For ResNet, two results corresponding to the two different difficulty levels (ResNet-1 and ResNet-2) are illustrated.

Discussion

Removing motion artifacts from 2D-Shepp-Logan phantom images seems to work reliably using pix2pix. However, it is possible that the network learnt the shape of the phantom and consequently, extracted it from the corrupted images (Fig. 2). For the MR brain images, both networks correctly removed the motion artifacts, but could not consistently reconstruct the images with all of their details. MSE values decrease after the application of the neural nets, Fig. 3. This is in agreement with the visual comparison, where most of the motion artifacts are removed from the corrupted images, but again, in case of a heavy corruption level, the network is not able to retrieve back all the edge information and the small structures are not visible, see Fig. 2. The DICE coefficients and the volume ratios, on the other hand, indicate a good agreement between the segmentation of the corrected and the ground-truth images, Fig. 3. ResNet-1 provides the best results with the lowest MSE values, the highest DICE coefficient, and almost 0.8 and 1.0 mean value for the volume ratio, Fig. 3. After increasing the difficulty level, the result slightly deteriorates, but still, ResNet-2 outperforms pix2pix.

Conclusion

Qualitative and quantitative assessments showed that the chosen networks are able to remove motion artifacts up to a certain level of corruption. While the results are encouraging, it remains a challenge to determine good hyperparameters of the networks and their training. In a comparison of ResNet and pix2pix, ResNet outperformed pix2pix.

Acknowledgements: This work was supported by the federal state of Saxony-Anhalt under grant number "I 88" (MedDigit); and was in part conducted within the context of the International Graduate School Memorial at OvGU (project no. ZS/2016/08/80646).

Selected References:

[1] Soumick Chatterjee et al. "A deep learning approach for reconstruction of undersampled Cartesian and Radial data". In: Oct. 2019.

[2] Lee R. Dice. "Measures of the Amount of Ecologic Association Between Species". In: *Ecology* 26.3 (1945), pp. 297–302. DOI: 10.2307/1932409. eprint: https://esajournals.onlinelibrary.wiley.com/doi/pdf/10.2307/1932409. URL: https://esajournals.onlinelibrary.wiley.com/doi/abs/10.2307/1932409.

[3] F. Godenschweger et al. "Motion correction in MRI of the brain." eng. In: *Physics in medicine and biology* 61 (5 Mar. 2016), R32–56.

[4] P. Isola et al. "Image-to-Image Translation with Conditional Adversarial Networks". In: *2017 IEEE Conference on Computer Vision and Pattern Recognition (CVPR)*. July 2017, pp. 5967–5976.

[5] Wenhao Jiang et al. "Respiratory Motion Correction in Abdominal MRI using a Densely Connected U-Net with GAN-guided Training". In: *ArXiv* abs/1906.09745 (2019).

[6] Thomas Küstner et al. "Retrospective correction of motion-affected MR images using deep learning frameworks". In: *Magnetic Resonance in Medicine* 82.4 (2019), pp. 1527–1540. DOI: 10.1002/mrm.27783.

[7] Ilkay Oksuz et al. "Cardiac MR Motion Artefact Correction from K-space Using Deep Learning-Based Reconstruction". In: *Machine Learning for Medical Image Reconstruction*. Ed. by Florian Knoll, Andreas Maier, and Daniel Rueckert. Cham: Springer International Publishing, 2018, pp. 21–29. ISBN: 978-3-030-00129-2.

[8] Muhammad Usman et al. "Motion Corrected Multishot MRI Reconstruction Using Generative Networks with Sensitivity Encoding". In: *ArXiv* abs/1902.07430 (2019).

[9] Maxim Zaitsev, Julian Maclaren, and Michael Herbst. "Motion artifacts in MRI: A complex problem with many partial solutions." eng. In: *Journal of magnetic resonance imaging : JMRI* 42 (4 Oct. 2015), pp. 887–901.